Polarization Resolved Four-Wave-Mixing-Based Measurement in Bulk Material Semiconductor Optical Amplifier

F. Surre[a], B. Kennedy[a,b], P. Landais[a], *Member, IEEE,* S. Philippe[c], A.L. Bradley[c]
[a] *Research Institute for Networks and Communications Engineering, Dublin City University, Dublin 9, Ireland*
[b] *Departamento de Ingenieria Electrica, Universidad de Santiago, Chile*
[c] *Semiconductor Photonics, Trinity College Dublin, Ireland*
Tel: +353 17008044, Fax: +353 17005508, e-mail: surref@eeng.dcu.ie

ABSTRACT

The anticipated growth in demand for bandwidth leads to the development of all-optical signal processing techniques at ever increasing data rates. One possible candidate to achieve the required performance is the semiconductor optical amplifier (SOA). It has been demonstrated that ultra-fast gain processes are dominant for pulsewidths below 10 ps.

In this paper we present experimental results on the polarization dependence of ultra-fast gain dynamics in InGaAsP/InP bulk material SOA probed using a four-wave mixing technique. Using a standard low-pass filter model it is possible to retrieve information on the polarization dependence of linewidth enhancement factors and the timescales for non-linear phenomena such as carried density pulsation and carrier heating.

Keywords: semiconductor optical amplifier, four-wave-mixing, carrier density pulsation, carrier hearing.

1. INTRODUCTION

All-optical signal processing techniques using Semiconductor Optical Amplifiers (SOAs) such as cross-gain modulation, cross-phase modulation and four-wave mixing (FWM) continue to be developed [1]. The anticipated growth in demand for bandwidth leads to the development of these systems at ever increasing data rates. This means that the gain of the SOA must be modulated on smaller and smaller timescales. It has been demonstrated that the ultra-fast gain processes are dominant for pulsewidths below 10 ps [2]. The level of polarization dependence introduced by these ultra-fast gain processes has been treated theoretically on sub-picosecond pulses [3] and [4]. However it has not been demonstrated or investigated for picosecond pulses. The purpose of our paper is to experimentally investigate the polarization dependence of ultra-fast gain process in SOA. Such dependence will impact on the operation of optical systems.

The results presented in this paper quantify the effects of the polarization dependence of the carrier density pulsations (CDP) and carrier heating (CH) processes using a four-wave-mixing based experimental setup. A variation in the detuning between pump and probe signals injected into the device allows the gain to be modulated at different frequencies. It is then possible to fit this experimental data to a theoretical expression in order to retrieve the carrier recovery time and linewidth enhancement factor, α associated with each process. It is possible to obtain polarization resolved results by varying the polarization of the injected pump and probe signals.

This paper is organized as follows: In Section 2 the FWM setup and results are presented, in Section 3 an interpretation of the results is given, and finally in Section 4 conclusions are drawn.

2. FWM EXPERIMENT AND RESULTS

The SOA under test is commercially available from Avanex under reference A1901. It is a 300 µm tensile strained InGaAsP bulk active waveguide device, terminated by 150 µm lateral tapered active regions. It is biased at 200 mA and temperature controlled at 23 °C. Its gain peak is at 1535 nm and a fibre-to-fibre gain of 24 dB at 200 mA can be achieved.

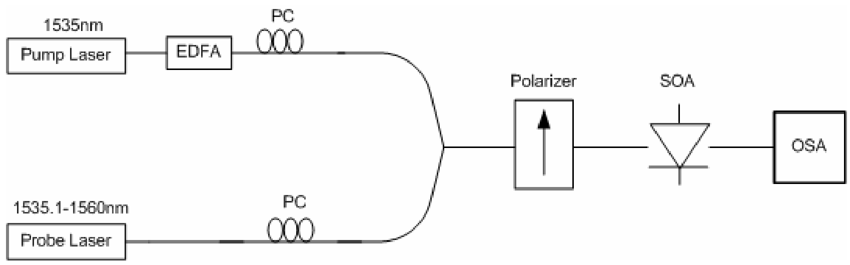

Figure 1. FWM setup.

The work reported in this paper was supported by Enterprise Ireland proof of concept grant POC/2004/331

Two signals called the pump and the probe at frequencies f_p and f_s, respectively are launched into the semiconductor optical amplifier. Due to the third order non-linear effect of the semiconductor material, these signal beat together generating a modulation of the complex refractive index of the waveguide at the frequency detuning $\Omega = |f_s - f_p|$. This lead to a generation of waves separated spectrally by Ω. Five FWM processes contribute to this wave generation, CDP which is an interband effect, CH, spectral-hole-burning (SHB), two-photon absorption (TPA), and the Kerr effect which are intraband effects. The first three processes are stronger than the last two for Ω less than 8 THz. For smaller values of Ω, CDP is the most efficient effect. As Ω increases, the efficiency of CDP reduces as it cannot follow the modulation and CH starts to be the most efficient effect. As Ω increases further, SHB will dominate. Varying Ω makes possible the observation to the contribution of each of the nonlinear gain processes [5-9]. We propose to use this technique to measure the polarization dependence of CDP and CH processes.

Two external cavity tunable CW lasers are used to perform the FWM experiment as depicted in Fig. 1. The wavelength of the pump is 1535 nm, which is within the 3 dB gain bandwidth of the device. The wavelength of the probe is varied from 1535 nm to 1560 nm in steps as low as 0.1 nm. Ideally it would be preferable to have the pump wavelength closer to the gain peak of the device, which occurs at 1515 nm, but there is a restriction due to the EDFA which does not amplify the signal significantly, below 1535 nm. The EDFA is required to amplify the pump signal, as a strong intensity is necessary in order to suppress the gain of the device. The choice of wavelengths used for the pump and the probe thus involves a trade-off between the gain spectrum of the EDFA, which operates in the C-band, and the gain spectrum of the SOA. In this experiment, with the frequency detuning available, measurements of time-varying phenomena recovering on timescales greater than 300 fs can be achieved. The pump power is maintained at 9 dBm for all measurements, whilst the probe power is constant at -4 dBm. A difference of 13 dB between the powers of the pump and the probe is selected to produce the maximum value for the conversion efficiency [9], defined by:

$$\rho_{\mathrm{exp}} = \frac{\mathrm{P_{conj}}}{\mathrm{P_{probe}}} \tag{1}$$

where P_{conj} is the power of the symmetric signal of the probe with respect to the pump signal, and P_{probe} the probe power. Both powers are measured at the SOA output. An optical spectrum analyser (OSA) with a resolution bandwidth of 0.07 nm is used to measure these output powers. The polarization of both the pump and the probe is controlled using a polarizer and a polarization controller (PC). The polarizer ensures that: i) both signals are linearly polarized, ii) they are co-polarized, a requirement for efficient FWM, and iii) they are injected along the same axis of the PM lensed fibre. The angle, θ between the co-polarized pump and probe signals and the TE axis of SOA (aligned along the plane of the active layer) is varied with respect to the axis of the device by physically rotating the PM lensed fibre. The coupling from the lensed fibre to the SOA is maintained at a constant level as the polarization is varied and in both arms PCs are used to align signals along the axis of polarizer maintaining constant probe and pump powers. The conversion efficiency is recorded as a function of wavelength detuning between the pump and the probe for each value of θ.

The conversion efficiency can be expressed theoretically as follows:

$$\rho_{th} = S_0^2(L)\,|\,f_{cdp}(\Omega) + f_{ch}(\Omega)\,|^2 \tag{2}$$

where S_0 represents the pump photon density. The contributions from carrier density pulsations (f_{cdp}) and carrier heating (f_{ch}) are defined as follows [10]:

$$f_{cdp}(\Omega) = -\frac{1}{S_{sat}}\frac{1 - j\alpha_{cdp}}{2(1 - j2\pi\,\Omega\tau_{cdp})} \tag{3}$$

$$f_{ch}(\Omega) = -\frac{1}{S_{ch}}\frac{1 - j\alpha_{ch}}{(1 - j\,2\pi\Omega\tau_{ch})(1 - j\,2\,\pi\Omega\tau_{shb})} \tag{4}$$

where the α_i, τ_i and S_i parameters refer to the linewidth enhance factors, carrier recovery times and characteristic power associated with each process respectively. By fitting the efficiency data it is possible to retrieve the above parameters related to CDP and CH as a function of the angle of θ. The SHB is neglected as the detuning range is limited to 3.5 THz, corresponding to a time resolution of approximately 300 fs, which is larger than the characteristic time of SHB. Above this detuning, a polarization dependence of the efficiency will occur [11] and therefore we work at lower detunings than this. Secondly, the spectral dependence of the gain can be neglected [12]. For Ω range of less than 3.5 THz the gain varies by less than 1 dB. Thirdly, the value for S_0 is also fixed as the pump signal is maintained at a constant power for all measurements.

The next step involves using a minimization technique in order to minimize the error between the experimental efficiency data and the theoretical efficiency, defined by Eqns. (3) and (4). The parameters in these equations are given initial values and six of these parameters are set as variables in order to reduce the error between the experimental and theoretical efficiency. This fitting is performed as a function of angular frequency detuning for the following parameters: S_{sat}, α_{cdp}, τ_{cdp}, S_{ch}, α_{ch} and τ_{ch}. The final values extracted are within the range of values found in the literature for these parameters.

The experimental efficiency and the fitted efficiency are plotted as a function of Ω in Fig. 2 for θ at 30°, together with the calculated contribution from CDP and CH. The accuracy of the fitting can be seen on the graph. For a small frequency detuning CDP has the largest effect on the efficiency, as expected. As Ω is increased, the CDP decreases by approximately 20 dB/decade, and the CH contribution becomes more important.

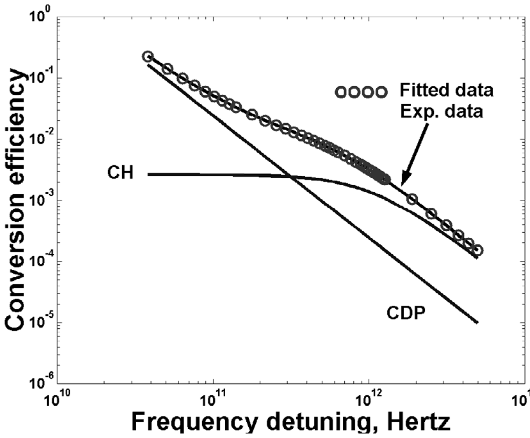

Figure 2. Conversion efficiency as a function of frequency detuning. Experimental data (o) and fitted curves for CDP and CH processes at θ = 30°.

The fitting is performed for a range of injection polarizations between -30° and 90°. The accuracy of the fitting may be gauged by considering the variance between the experimental data and the fitted data. The variance calculated for each angle of polarization is less than 0.001%. Fig. 3*a* shows the extracted values for α_{cdp}, and the carrier recovery time, τ_{cdp}, associated with CDP as a function of the polarization angle θ. α_{cdp} varies from a value of less than 4.5 at 30° up to a peak of 6.5 at 60°. Similarly the carrier recovery time varies from 50 ps to 230 ps. Fig. 3*b* shows α_{ch}, and the recovery time, τ_{ch}, associated with CH, as a function of polarization angle. The α_{ch} is approximately 1 at -30° and peaks at 60° with a value of approximately 3.

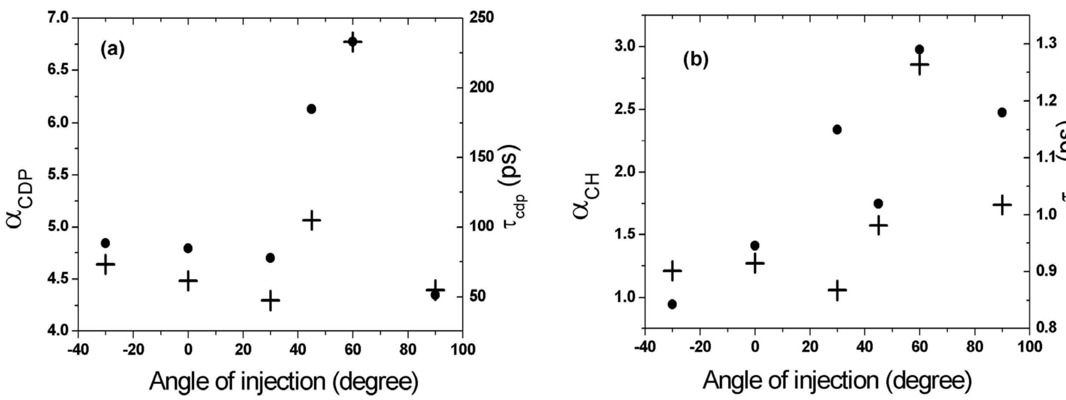

Figure 3. Linewidth enhancement factor (●) and recovery time (+) obtained from FWM experiment for both: (a) CDP and (b) CH as a function of angle of injection.

3. DISCUSSION

The FWM results presented in Fig. 3*a* and Fig. 3*b* showed a polarization dependence of the linewidth enhancement factors recovery times associated with CDP and CH. At θ = 60°, the largest values for recovery times of CDP and CH were measured and at θ = 30° the smallest values. These results indicate that the TM axis of the device could be shifted close to 60°. For a tensile strained bulk device there are more TM transitions than TE transitions due to the shifting of the sub-bands in the valence band [13]. The light holes, which give rise to TM transitions, are favoured under such strain. A larger TM gain and so a greater depletion of carriers for injected light polarized along the TM axis are achieved. So TM light results in a lower carrier density population, this leads to a longer carrier recovery time due to the fact that the carrier lifetime is inversely proportional to carrier density.

Further, due to the fact that the TM gain is higher than the TE gain in the tensile strained case, there would also be a larger shift towards lower wavelengths for the TM mode, as carriers in higher electron states would participate in the gain under such circumstances. As α_{cdp} is inversely proportional to the wavelength this implies that α_{cdp} would shift towards larger values for light polarized along the TM direction, as observed in Fig. 3*a*.

4. CONCLUSIONS

The polarization dependence of the gain dynamics in a bulk SOA has been measured using a CW FWM experimental setup. The gain recovery times and α-factors as a function of polarization for both the CDP and CH mechanisms were extracted. Both processes have shown polarization dependence with the minimum recovery time occurring for pump and probe signals with a linear state of polarization at 30° with respect to the plane of the active layer and a maximum recovery time for a state of polarization of 60°. The α-factors also showed polarization dependence, with peak values, of 6.5 and 3 for the CDP and CH respectively, also corresponding to 60°. Such polarization dependences must be taken into account for SOA applications in optical networks, as depending on the polarization angle, θ, different recovery times can be achieved and different spectral components can be added to the transmitted signal.

ACKNOWLEDGEMENTS

This work is supported by Enterprise Ireland.

REFERENCES

[1] A. Poustie, "Semiconductor devices for all-optical signal processing," Optical Communication, *ECOC 2005. 31st European Conference on,* vol. 3, 25-29, pp475-478, Sept. 2005.

[2] P. Borri, *et al.*, "Measurement and calculation of the critical pulsewidth for gain saturation in semiconductor optical amplifiers," *Optics Comms.*, vol. 164, pp. 52-55, June 1999.

[3] X. Yang, *et al.*, "Nonlinear polarization rotation induced by ultrashort optical pulses in a semiconductor optical amplifier," *Optics Comms.,* vol. 223, pp. 169-179, January 2003.

[4] Z. Li, *et al.*, "Simulation of mode-locking by nonlinear polarization rotation in a semiconductor optical amplifier," *IEEE J. Quant. Electron.,* vol. 41, pp. 808-816, June 2005.

[5] L. F. Temeijer, "Effects of nonlinear gain on four-wave mixing and asymmetric gain saturation in semiconductor laser amplifier," *Appl. Phys. Lett.,* vol. 59, pp.499-501, 1991.

[6] K. Kikuchi, *et al.*, "Analysis of origin of nonlinear gain in 1.5 um semiconductor active layers by highly nondegenerate four-wave mixing," *Appl. Phys. Lett.,* vol. 64, pp.548-550, 1994.

[7] A. Mecozzi, "Analytical theory of four-wave mixing in semiconductor amplifiers," *Opt. Lett.* vol.19, pp. 892-894, 1994.

[8] S. Diez, *et al*., "Four-wave mixing in semiconductor optical amplifiers for frequency conversion and fast optical switching," *IEEE J. Sel. Top. Quant.Electron.,* vol. 3, pp. 1131-1145, 1997.

[9] S. Scotti, *et al*., "Effects of ultrafast processes on frequency converters based on four-wave mixing in semiconductor optical amplifiers," *J. Sel. Top. Quantum Electronics,* vol. 3, no. 5, pp. 1156-1161, October 1997.

[10] A. Uskov, *et al.*, "Wave mixing in semiconductor laser amplifiers due to carrier heating and spectral-hole burning," *IEEE J. Quant. Electron.,* vol. 30, pp. 1769-1781, 1994.

[11] S. Diez, *et al.*, "Effect of birefringence in bulk semiconductor optical amplifiers on FWM," *IEEE Photon. Technol. Lett.,* vol. 10, pp. 212-214, 1998.

[12] K. Obermann, *et al.*, "Noise analysis of frequency converters utilizing semiconductor laser amplifiers," *IEEE J. Quant. Electron.,* vol. 33, pp. 81-88, 1997.

[13] E. P. O'Reilly et al., "Band-structure engineering in strained semiconductor lasers," *IEEE J. Quant. Electron.* vol. 30, pp. 366-379, 1994.